Anions Stabilize a Metarhodopsin II-like Photoproduct with a Protonated Schiff Base†

Reiner Vogel,‡,§ Gui-Bao Fan,§,|| Friedrich Siebert,*,‡ and Mordechai Sheves*,||

Biophysics Group, Institut für Molekulare Medizin und Zellforschung, Albert-Ludwigs-Universität Freiburg, Albertstrasse 23, D-79104 Freiburg, Germany, and Department of Organic Chemistry, Weizmann Institute of Science, Rehovot 76100, Israel

Received June 29, 2001; Revised Manuscript Received August 23, 2001

ABSTRACT: In rhodopsin, the retinal chromophore is covalently bound to the apoprotein by a protonated Schiff base, which is stabilized by the negatively charged counterion Glu^{113}, conferring upon it a pK_a of presumably >16. Upon photoexcitation and conformational relaxation of the initial photoproducts, the Schiff base proton neutralizes the counterion, a step that is considered a prerequisite for formation of the active state of the receptor, metarhodopsin II (MII). We show that the pK_a of the Schiff base drops below 2.5 in MII. In the presence of solute anions, however, it may be increased considerably, thereby leading to the formation of a MII photoproduct with a protonated Schiff base (PSB) absorbing at 480 nm. This PSB is not stabilized by Glu^{113}, which is shown to be neutral, but by stoichiometric binding of an anion near the Schiff base. Protonation of the Schiff base in MII changes neither coupling to G protein, as assessed by binding to a transducin-derived peptide, nor the conformation of the protein, as judged by FTIR and UV spectroscopy. A PSB and an active state conformation are therefore compatible, as suggested previously by mutants of rhodopsin. The anion specificity of the stabilization of the PSB follows the series thiocyanate > iodide > nitrate > bromide > chloride > sulfate in order of increasing efficiency. This specificity correlates inversely with the strength of hydration of the respective anion species in solution and seems therefore to be determined mainly by its partitioning into the considerably less polar protein interior.

Rhodopsin is the light receptor responsible for dim vision in rod photoreceptor cells (*1*, *2*). It is an integral membrane protein consisting essentially of seven membrane-spanning helices forming a bundle structure, interconnected by extracellular and cytoplasmic loops, as is evident from projection maps (*3*) and the recently published three-dimensional (3D) crystal structure (*4*). The light sensitive prosthetic group of rhodopsin in the unphotolyzed dark state is 11-*cis*-retinal, which is covalently bound to Lys^{296} on helix 7 via a protonated Schiff base and entirely surrounded by the apoprotein (opsin) forming the retinal binding pocket. In vertebrate rhodopsins, the charge of the protonated Schiff base linkage in the dark state is compensated by a negatively charged counterion on helix 3, Glu^{113} in bovine rhodopsin (*5*, *6*). Photolysis of the dark state leads to the isomerization of the retinal chromophore from an 11-*cis* to an *all-trans* geometry. Subsequent structural changes of the protein and deprotonation of the Schiff base then lead within milliseconds to the formation of the active state metarhodopsin II (MII,[1] $\lambda_{max} = 380$ nm), which activates G protein and initiates visual signal transduction. Metarhodopsin I (MI, $\lambda_{max} = 480$ nm), a still inactive precursor of MII, is in equilibrium with the active state, MII. This equilibrium is shifted toward MII by decreasing the pH, by increasing the temperature or fluidity of its immediate environment (*7*, *8*), or by binding to its cognate G protein transducin or to peptides mimicking the binding domains of transducin (*9*, *10*).

Retinal and the apoprotein opsin do not form two separate entities, but are strongly interacting. In the dark state, retinal interacts tightly with the helix bundle and drives after photoisomerization to *all-trans*-retinal the protein to the active state conformation, thus enabling the docking of downstream signaling elements (*1, 11*).

On the other side, the protein environment of the retinal binding pocket also changes the properties of the chromophore itself. Retinal Schiff bases absorb in polar solvents at ∼380 nm in their unprotonated form and at ∼440 nm if they are protonated. Rhodopsin in the unphotolyzed dark state has its absorption maximum at 500 nm, the 60 nm red shift from a protonated Schiff base (PSB) in solution being due to protein−chromophore interactions, which is termed the opsin shift. Studies on model Schiff bases in solution suggested that the red shift of the chromophore may be due to an increased distance between the Schiff base proton and its counterion, which is weakening their electrostatic interac-

† This work was supported by grants from Deutsche Forschungsgemeinschaft (Grant VO 811/1-1 to R.V. and Grant SI 278/16-3,4 to F.S.), by Fonds der Chemischen Industrie (to F.S.), by the A. M. N. Fund for the Promotion of Science, Culture and Arts in Israel (to M.S.), by the US−Israel Binational Science Foundation (to M.S.), and by the Israel National Science Foundation administered by the Israel Academy of Sciences and Humanities (to M.S.).

* To whom correspondence should be addressed. F.S.: Institut für Molekulare Medizin und Zellforschung, Albert-Ludwigs-Universität, Albertstr. 23, D-79104 Freiburg, Germany; phone, +49 761 203 5396; fax, +49 761 203 5399; e-mail, frisi@uni-freiburg.de. M.S.: Department of Organic Chemistry, Weizmann Institute of Science, Rehovot 76100, Israel; phone, 972 8 9344320; fax, 972 8 9344142; e-mail, mudi.sheves@weizmann.ac.il.

‡ Albert-Ludwigs-Universität Freiburg.

§ Both authors contributed equally.

|| Weizmann Institute of Science.

[1] Abbreviations: MI, metarhodopsin I; MII, metarhodopsin II; PP, photoproduct; SB, Schiff base; PSB, protonated Schiff base; FTIR, Fourier transform infrared spectroscopy; ATR, attenuated total reflectance; MES, 2-(*N*-morpholino)ethanesulfonic acid; MOPS, 3-(*N*-morpholino)propanesulfonic acid; BTP, bis-tris propane.

10.1021/bi0113667 CCC: $20.00
Published on Web 10/13/2001

tion (*12*, *13*). Even more striking than its influence on the wavelength, however, is the effect of the protein environment on the apparent pK_a of the Schiff base (see ref *14* for a recent review), which shifts from ~7 in solution to presumably >16 in the dark state of rhodopsin, as determined using retinal analogues (*15*). It was suggested that the high pK_a of the protonated Schiff base is attributed to a specific geometrical arrangement of the Schiff base and its counterion allowing an efficient bridging of water molecule that stabilizes the ion pair (*16*). This proposal is in keeping with the observation that in the dark state of rhodopsin mutants with the native, negatively charged counterion Glu^{113} replaced with an uncharged residue (*5*, *6*), the pK_a of the Schiff base drops from >16 to well below 5 in the absence of solute anions. Interestingly, a PSB can be restored in the dark state of these mutants by offering solute anions, which may then serve as an artificial counterion in the protein (*17*, *18*).

In the past decade were found several rhodopsin mutants (see ref *19* for a summary) as well as a pigment with a modified chromophore (*20*) that are able to form an active state without deprotonation of the Schiff base. These discoveries have shed some more light on the involved proton transfer reactions required for formation of the active state (*20*, *21*). In all of these pigments, the amino acid at position 113, corresponding to the native counterion, is very likely neutral in the active state, a requirement met by all mutants of rhodopsin examined in this respect to date. A necessary step in the activation of rhodopsin could therefore be the neutralization of the charge of Glu^{113} by proton transfer from the Schiff base (*19*), which is also in agreement with results from invertebrate rhodopsins where the corresponding residue is neutral (*22*). After this necessary proton transfer step, the protonation state of the Schiff base is in this picture not relevant for the active state. This notion does not contradict results from active site-methylated rhodopsin, which has no transferable Schiff base proton, and which does not support the formation of the active state (*23*, *24*). Therefore, if the local environment around the Schiff base is changed in the active state of a modified pigment compared to the MII state of native rhodopsin, or if there is a counterion different from Glu^{113} available, which may stabilize a positively charged Schiff base within the protein, a PSB and an active conformation do not need to be contradictory.

In this study, we show for the first time that the Schiff base in native MII is titratable in the presence of solute anions. A MII state with a protonated Schiff base absorbing at ~480 nm (in the following MII_{PSB}, in contrast to the "normal" MII state with a deprotonated Schiff base, MII_{380}) is stabilized upon stoichiometric binding of an anion near the Schiff base thus serving as an artificial counterion. The anion specificity for the stabilization of this novel state follows the series sulfate < chloride < bromide < nitrate < iodide < thiocyanate in order of increasing efficiency. This series correlates inversely with the strength of the ion−water interaction of the respective species in solution and reflects therefore its ability to enter a less polar environment (*25*), e.g., the interior of a protein, a step which requires the anion to abstract at least part of its hydration shell.

EXPERIMENTAL PROCEDURES

Preparation of the Pigment. Bovine rhodopsin from rod outer segments was prepared from cattle retinae in its native disk membrane environment essentially as described previously (*26*). For measurements with the purified pigment in detergent, rhodopsin was purified on a concanavalin A Sepharose column (Pharmacia Biotech, Uppsala, Sweden) in dodecyl maltoside (Biomol, Hamburg, Germany) (*27*). To monitor UV changes of MI in detergent, rhodopsin in membranes was dissolved in 2% digitonin (Merck, Darmstadt, Germany) and insoluble matter was removed by centrifugation. To assess the vibrational bands of the chromophore and to determine its intrinsic pK_a, rhodopsin was regenerated as described previously (*20*) with 9-*cis*-retinal isotopically labeled with ^{13}C at positions C-14 and C-15 (a generous gift from J. Lugtenburg, Leiden University, Leiden, The Netherlands) or with 9-*cis*-14-fluororetinal (*15*). All experiments involving pigments were carried out under dim red light, and samples were stored in distilled water or 1 mM phosphate buffer at −20 °C.

UV−Visible Spectroscopy. UV−visible spectroscopy was performed with a Perkin-Elmer Lambda 17 UV−vis spectrophotometer equipped with a thermostated cuvette holder (stability within ±0.2 °C) in 100 μL microcuvettes with a 10 mm path length (Hellma, Müllheim, Germany). Unless stated otherwise, all UV−vis measurements were carried out at 10 °C to prevent thermal decay of the MII photoproduct during the experiment. We used citric acid, MES, MOPS, and bis-tris propane (BTP) as buffers in overlapping pH ranges at a concentration of 20 mM unless stated differently. The scanning speed was set to 960 nm/min, and the acquisition time was therefore less than 1 min. After a dark state spectrum had been recorded, the sample was illuminated for 20 s with a fiber optic fitted to a 150 W halogen lamp equipped with an OG 530 cutoff filter (Schott, Mainz, Germany). After illumination, subsequent photoproduct spectra were taken to verify the thermal stability of the photoproduct. For measurements in membranes, we used an identical but bleached sample as a blank in the reference beam to account for the considerable light scattering in the sample. Measurements in detergent were carried out in 0.1% dodecyl maltoside. For UV spectroscopy of the MI state, 2% digitonin was used instead.

Quantitative Determination of the Schiff Base Protonation State. All quantitative measurements relating to Schiff base protonation were performed with UV−vis spectroscopy. We determined the amount of MII with the protonated Schiff base by forming the photoproduct minus dark state difference spectrum and determining the position of the negative rhodopsin depletion peak, which is found at ~500 nm in the absence of MII_{PSB} and which shifts to longer wavelengths with increasing MII_{PSB} contributions. The peak position was determined from the first derivative of the smoothed difference spectrum. Next, we also determined the peak positions for the limiting cases with either no MII_{PSB} or no MII_{380}, and calculated the amount of MII_{PSB} divided by the amount of total photoproduct (MII_{380} + MII_{PSB}) by a linear interpolation for the intermediate cases. As this method depends on the position of the MII_{PSB} peak, we had to make sure that this position is not dependent on the anion species; otherwise, the method would have to be adjusted for each anion species separately. We found in our experiments, however, no significant and reproducible anion specificity of the position of the absorption peak of MII_{PSB}. We used therefore for all anions the following interpolation to determine the amount

of MII_{PSB} from the position of the depletion peak λ_D: $MII_{PSB}/(MII_{380} + MII_{PSB}) = (\lambda_D - \lambda_0)/(\lambda_1 - \lambda_0)$, where λ_0 and λ_1 are the respective values for zero and full MII_{PSB} formation, respectively. In dodecyl maltoside, the respective values were determined to be 500 and 532 nm for λ_0 and λ_1, respectively, and in membranes 504 and 535 nm, respectively. The slight red shift of the limiting values in membranes is presumably due to the differing environment and slight contribution of isorhodopsin ($\lambda_{max} = 490$ nm) or other *cis* species being formed in membranes in addition to MII. In initial experiments, we also determined explicitly absorption changes at 380 and 480 nm and normalized these by the amount of photolyzed pigments. The obtained results were found to correspond to those obtained with the difference spectrum approach.

The obtained values for MII_{PSB} were fitted by a Henderson−Hasselbalch equation with one pK_a (in the case that only MII_{PSB} and MII_{380} were produced)

$$MII_{PSB}/(MII_{380} + MII_{PSB}) = 10^{pK_a - pH}/(1 + 10^{pK_a - pH})$$

The difference spectra for the MII precursor MI ($\lambda_{max} = 480$ nm), which also has a protonated Schiff base, and MII_{PSB} are hardly distinguishable due to the similar positions of their absorption maxima and the only small difference in their spectral widths (that of MII_{PSB} is slightly wider). Due to this coincidence, it is possible to determine the amount of MI with the same method that was used for MII_{PSB}. In the case of a contribution by both species, we determined the amount of photoproduct with protonated Schiff base PP_{PSB}, i.e., MII_{PSB} and MI, divided by the amount of total photoproduct (MI + MII). The obtained data were then fitted to the sum of two Henderson−Hasselbalch equations with pK_1 and pK_2 for the transition from MII_{PSB} to MII_{380} and from MII to MI, respectively

$$PP_{PSB}/PP_{total} = 10^{pK_1 - pH}/(1 + 10^{pK_1 - pH}) + 1 - 10^{pK_2 - pH}/(1 + 10^{pK_2 - pH})$$

thus allowing a distinction between MI and MII_{PSB} based on their opposite pH dependency.

Another possibility for determining the MII_{380}/MII_{PSB} ratio and thus the pK_a of the transition was to determine by difference spectra the fraction of MII_{380} formation that occurredimmediately after pigment illumination. In the subsequent thermal decay of both MII states, we followed the decay of MII_{PSB} to determine thereby its fraction in the mixture. This method (decay method) was applied to the titration of 14F-pigment in digitonin at 22 °C. Under these conditions, a slightly lower MII_{PSB} contribution was observed compared to those from other experiments carried out at 10 °C.

FTIR Spectroscopy. To determine the conformational properties of the different photoproduct species, we performed infrared measurements with a Bruker IFS 28 FTIR spectrometer, equipped with a liquid nitrogen-cooled HgCdTe detector. We recorded several blocks of 512 scans at 4 cm^{-1} resolution (acquisition time of 60 s each) before and after sample illumination (as described for UV−vis spectroscopy). The blocks recorded before illumination were used for baseline corrections, and the subsequent blocks recorded after illumination were examined for photoproduct decay.

FTIR samples were prepared by drying 1.0−1.5 nmol of rhodopsin in membranes onto a 7 mm wide round spot of a specially designed CaF_2 window, separated from its 4 μm higher rim by a depression that was ~1 mm wide. The sample was hydrated with 1 μL of the desired buffer/salt solution, sandwiched with a second CaF_2 window, and mounted to a thermostated sample holder in the measuring chamber. In these sandwich samples, only the 4 μm thin sample area irradiated by the infrared beam was in contact with the excess buffer being pressed into the surrounding depression thus forming a reservoir to enhance buffer capacity. The pH adjustment was found to be accurate down to pH 5. At lower pH values, the buffer capacity was not sufficient to bring the sample to the adjusted pH value of the buffer (as verified by ATR spectroscopy). In this range, therefore, the pH value of the samples can only be estimated. The accuracy of pH adjustment could be extended to a lower pH range by reducing the sample amount to 0.5 nmol or by increasing the buffer concentration. On the other hand, as exact knowledge of the pH was not as important as a high signal-to-noise ratio and only little influence of the buffer anion on the results, the strategies were not pursued. In general, we therefore used 100 mM buffer of the same type that was used in UV−vis spectroscopy.

Peptide binding was assayed in samples obtained by drying 20 nmol of the transducin-derived peptide analogue together with 0.5 nmol of pigment in membranes on the sample bottom window and rehydration with 200 mM citrate buffer containing 100 mM NaSCN.

RESULTS

Anion-Dependent Formation of a MII Photoproduct with a Protonated Schiff Base. The active rhodopsin photoproduct MII (deprotonated Schiff base, $\lambda_{max} = 380$ nm) is in native membranes in a pH-dependent equilibrium with its still inactive immediate precursor MI (protonated Schiff base, $\lambda_{max} = 480$ nm), which is preferentially formed at higher pH (*7*). In addition to this well-established equilibrium, a second transition of MII can be observed toward lower pH values in the presence of solute anions. This new acidic species is absorbing maximally at ~480 nm, suggesting a protonated Schiff base. It is in a pH-dependent equilibrium with the normal MII photoproduct with a deprotonated Schiff base, as shown in Figure 1, and can be observed both with rhodopsin in native membranes and with detergent-solubilized rhodopsin. In the sections below, we will show that, despite having a protonated Schiff base, this photoproduct is not related to MI, which is formed at the high end of the pH spectrum. Instead, the existence of this species at the opposite end of the pH range reflects an internal protonation equilibrium of the Schiff base in MII, which is directly related to the external pH and to the solvent concentration of anions. As we will show that this species shares a protein conformation and coupling to transducin-derived peptides with classical MII, we will term it in anticipation MII with protonated Schiff base, MII_{PSB}, in contrast to classical MII with a deprotonated Schiff base (in the following MII_{380}). We use the term MII therefore not in a strictly spectroscopic sense, which reserves the terminology MII to the 380 nm species, but in a functional sense. In this sense, MII describes the active rhodopsin photoproduct, thus representing a distinct protein conformation capable of coupling to G protein.

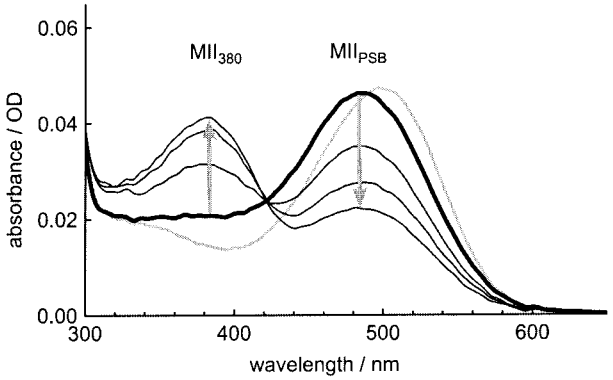

FIGURE 1: Reversibility of the formation of a MII photoproduct with a protonated Schiff base. Rhodopsin forms in the presence of 4 M NaCl at pH 3.5 a photoproduct with a protonated Schiff base and a λ_{max} of ~480 nm (gray line, dark state; thick black line, photoproduct). Upon repeated addition of small amounts of dilute NaOH, this photoproduct can revert to normal MII with a deprotonated Schiff base and a λ_{max} of 380 nm (thin black lines, final pH of 4.5). Acidification with concentrated HCl to pH 1 at the end of the experiment to trap photoproduct with an intact retinal Schiff base revealed no significant hydrolysis of the Schiff base during the measurements. The experiment was carried out with purified pigment in detergent at 10 °C.

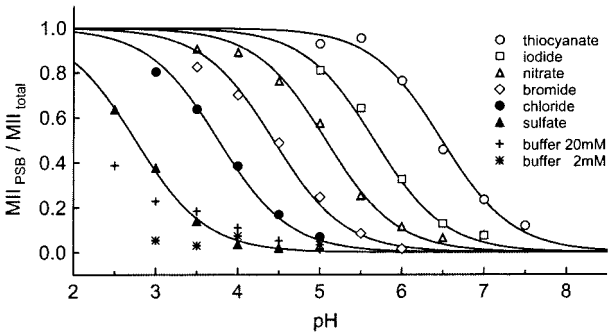

FIGURE 2: Dependence of the apparent pK_a of the Schiff base of MII on the anion species. The contribution of MII with a protonated Schiff base to the amount of total MII photoproduct was determined in the presence of the respective anion (1 M) as a sodium salt. The experiments were carried out with pigment in its native membrane environment for higher photoproduct stability against high salt and low pH at 10 °C. We used 20 mM buffer throughout (see Experimental Procedures) except for the experiments at low pH with sulfate and chloride, where the buffer concentration was reduced to 2 mM to minimize binding of the buffer anion (in this case, dihydrogen citrate) to the Schiff base. The effects of 20 and 2 mM citrate buffer alone are shown as well. The solid lines are fits to the Henderson−Hasselbalch equation with a single pK_a (see Table 1 for the determined values).

The pH dependence of the transition from MII_{380} to MII_{PSB} is ion specific, as shown in Figure 2, where we plot the fraction of MII with a protonated Schiff base over pH in the presence of 1 M salt. The data in Figure 2 were obtained from light-induced UV−vis difference spectra from rhodopsin in its native membrane environment and were evaluated as described in Experimental Procedures. The data are in agreement with the solid lines, which are fits to a Henderson−Hasselbalch equation with one pK_a (Table 1; see also Experimental Procedures).

It is therefore reasonable to conclude that the transition from MII_{380} to MII_{PSB} requires the uptake of one proton, and that the pK_a is the respective apparent acid constant of the Schiff base in MII, which is increased by the presence of salts. The apparent pK_a values obtained from the fits are shown in Table 1 both for rhodopsin in membranes and for purified rhodopsin in the detergent dodecyl maltoside. Interestingly, the salt specific pK_a values are very similar for both sample types. In contrast to this, the temperature and pH dependence of the transition from MI to MII, which is known to involve conformational changes of the protein, depends considerably on the fluidity of the embedding matrix (*8*). We can therefore conclude that major conformational changes of the protein are not involved in the transition from MII_{380} to MII_{PSB}.

Table 1: Salt Dependence of the pK_a Values of the Schiff Base in MII and Corresponding Dissociation Constants K_D[a]

	in membranes		in detergent	
salt	pK_a	K_D (μM)	pK_a	K_D (μM)
NaSCN	6.5	0.3	6.4	0.4
NaI	5.7	1.6		
$NaNO_3$	5.1	8		
NaBr	4.4	24	4.4	24
NaCl	3.8	160	3.6	250
$CaCl_2$			3.6	250
$MgCl_2$			3.6	250
Na_2SO_4	2.8	1800	2.6	2500
dihydrogen citrate[b]	–	60		
none[c]	<2.0	>15000		

[a] All data were determined at 10 °C with an anion concentration of 1 M in the native membrane environment or in the detergent dodecyl maltoside. The pK_a and K_D values are from least-squares fits of the data of Figure 2 and other data to a Henderson−Hasselbalch equation and to eq 4. The experimental error is estimated to be ±0.15 for the pK_a values, corresponding to approximately ±40% for the K_D values. [b] Determined in 200 mM citric acid buffer assuming a pK_a of 3.17 for the dissociation of citric acid. [c] Corresponding to the formation of MII_{PSB} in the absence of anion ($MII{\cdot}H^+$); for estimates, see the Supporting Information.

From Table 1, it is also evident that there is no cation specificity of the pK_a. Sodium, calcium, and magnesium chloride are all fit by the same pK_a. The observed protonation of the Schiff base in MII is therefore strictly anion specific.

Despite the observed anion specificity of the apparent pK_a of the Schiff base, we did not detect any significant influence of the anion species on the position of the absorption maximum of MII_{PSB}. This is in contrast to the effect of anions on the dark state of the counterion mutants of rhodopsin, E113Q and E113A, which show a protonated Schiff base only at low pH or in the presence of anions (*17*, *18*). There, the absorption maximum shifts appreciably, and is dependent on the anion species. In our case, a determination of a putative anion specificity of λ_{max} is somewhat hampered by the decreasing stability of the photoproduct at the low pH required with most anions to achieve quantitative conversion to MII_{PSB}. Still, we can estimate potential anion specific shifts of λ_{max} to be $\leq$ 5 nm.

It must be noted that the photoproducts were in general stable during the time required to record the photoproduct spectra at 10 °C. Only at the low-pH side of each titration curve, where the MII_{PSB}/MII_{total} ratio approaches 1, was some instability of the photoproduct observed, becoming noticeable by its absorption maximum moving slowly from 480 to 440 nm. With the difference spectrum method used for evaluation, a contribution of this slow blue shift to the initial photoproduct spectrum may slightly diminish the obtained values for MII_{PSB} and may therefore be responsible for the slight deviations of the data on the low-pH side of the titration curves from the fitted curve.

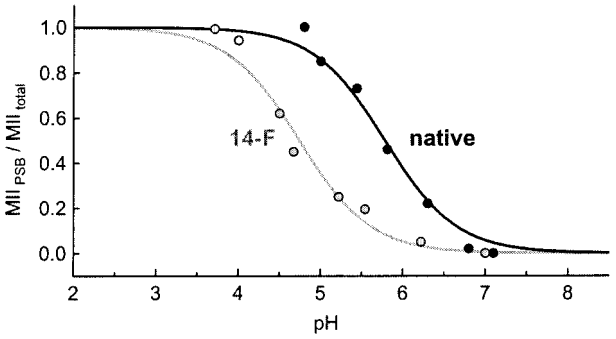

FIGURE 3: Titration of 14F-rhodopsin. The fraction of MII_{PSB} in native rhodopsin (black) and in 14F-rhodopsin (gray) was determined as described in Experimental Procedures in the presence of 1 M KSCN at 22 °C in 2% digitonin. The corresponding pK_a values of the Schiff base are under these conditions 4.7 and 5.8, respectively.

There is also some MII_{PSB} formation in the absence of explicitly added salt at very low pH, which is due to the anions of the employed 20 mM citrate buffer, as it vanishes upon decreasing the buffer concentration to 2 mM (Figure 1). All titration curves involving a very low pK_a were therefore obtained in 2 mM buffer.

Evidence for Direct Titration of the Schiff Base in MII. As a preliminary hypothesis, we assign the apparent pK_a observed for the titration of MII_{380} to MII_{PSB} to a simple equilibrium directly involving the Schiff base, i.e., $SB{\cdot}H^+ + H_2O \rightleftharpoons SB + H_3O^+$. However, in principle (e.g., if the Schiff base is inaccessible to H_3O^+ and OH^-), the observed equilibrium may not represent the direct titration of the Schiff base, but rather that of other putative groups in rhodopsin. Upon titration, such groups will induce protein conformational changes that perturb the active site by exposing the Schiff base and, thus, allow its deprotonation. This ambiguity can be resolved by using an artificial pigment derived from a retinal analogue which is fluorinated at C-14. Due to the stronger electronegativity of the fluoro substituent, the apparent pK_a of a 14F-retinal Schiff base is lowered by 2.2 units to 5.0 in a 1/1 ethanol/water solution, compared to 7.2 for a native retinal Schiff base (*15*).

Irradiation of the artificial pigment derived from 14F-retinal in the presence of 1 M NaSCN revealed that the pK_a of MII_{PSB} drops by 1.1 units relative to that observed for native rhodopsin under otherwise identical conditions (at 22 °C in 2% digitonin, the pK_a values were determined with the decay method; see Experimental Procedures), as shown in Figure 3. This observation implies that the intrinsic change induced in the pK_a of the free protonated Schiff base chromophore in solution is also reflected in that of the corresponding rhodopsin pigment. The differing 14F substitution effect in solution relative to that in the protein environment (2.2 and 1.1 pK_a units, respectively) may be due to different chromophore−protein interactions operating in the case of native retinal and the fluoro analogue. Direct evidence that the $MII_{380} \rightleftharpoons MII_{PSB}$ equilibrium is associated with the direct titration of the Schiff base nitrogen is thus provided.

MII_{380} and MII_{PSB} Are Equivalently Recognized by a Transducin-Derived Peptide. Rhodopsin's cognate G protein transducin, and several peptide mimics of the protein, are known to selectively bind and stabilize the active state MII at the expense of inactive conformations as MI (extra MII effect) (*9, 10*). We examined the influence on rhodopsin's photoproduct equilibria of a peptide analogue of the C-terminus of the transducin α-subunit, peptide 23 (Ac-VLEDLKSCGLF), which was recently found by screening of a combinatorial library and shown to bind and stabilize MII with high affinity (*28*). In Figure 4A, we examine the pH-dependent protonation of the Schiff base in the rhodopsin photoproducts in the presence of 100 mM NaSCN in membranes. In the absence of peptide (gray symbols), the classical MII_{380} with deprotonated Schiff base is formed only in a very narrow pH range around pH 6. With a pK of 5.4, it is in equilibrium with its acidic form (MII_{PSB}) that is formed at lower pH, while at pH 7.1, we observe the conformational transition to MI at alkaline pH. In agreement with previous studies (*28*), the presence of the peptide analogue (50 μM) has a strong influence on the MI ⇌ MII equilibrium and shifts the pK of the transition from 7.1 to >9 (black symbols). The internal MII protonation equilib-

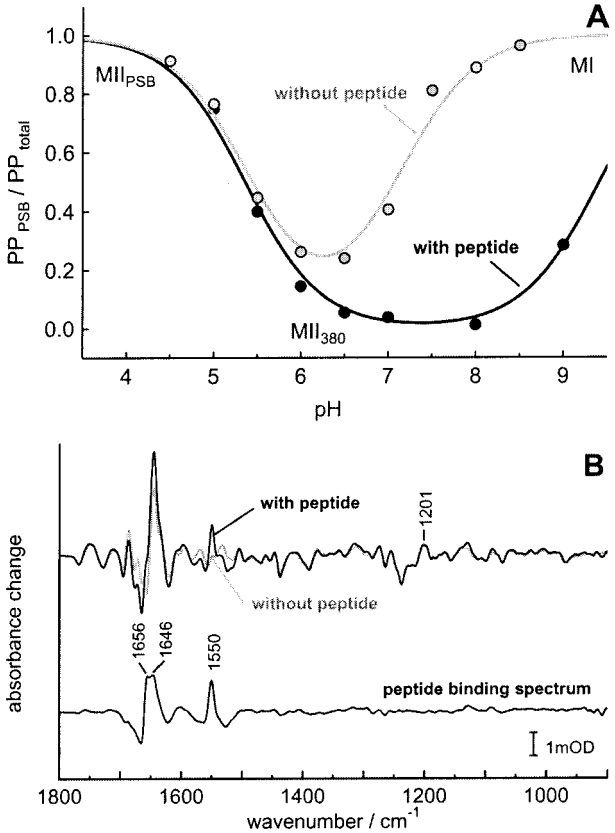

FIGURE 4: Transducin-derived peptide recognizes both MII_{380} and MII_{PSB}. (A) The effect of a high-affinity peptide analogue of the C-terminus of the transducin α-subunit on MII and MII_{PSB} was tested at 10 °C in 100 mM NaSCN with pigment in membranes. The presence of the peptide (50 μM) shifts the pK_a of the MI ⇌ MII equilibrium of rhodopsin (2.5 μM) from 7.1 to >9 by recognizing and stabilizing exclusively the active conformation of MII (extra MII effect). In contrast to this, the pK_a of the equilibrium between MII_{PSB} and MII_{380} is not affected (5.4), indicating that both species are recognized and stabilized equivalently by the peptide. (B) Binding of the peptide to MII_{PSB} was examined by infrared spectroscopy. The upper spectra are photoproduct minus dark state difference spectra of MII_{PSB} obtained in membranes at pH 4.5 in the presence of 100 mM NaSCN either in the presence (black) or in the absence (gray) of a 40-fold excess of peptide. In the lower spectrum, we formed the difference between both difference spectra. The resulting peptide binding spectrum therefore represents the changes involved in the transition from free MII_{PSB} with peptide to the MII_{PSB}−peptide complex.

rium between MII_{380} and MII_{PSB}, on the other hand, is unaffected by the presence of peptide. If the peptide had a preference for classical MII_{380} over MII_{PSB}, we would expect an extension of the pH range, in which MII_{380} is prevalent, toward lower pH values, in analogy to the effect on the MI ⇌ MII equilibrium. As this is not the case, we can conclude that both MII species are recognized by the peptide equivalently as active states irrespective of the Schiff base protonation state, while MI is not, and that binding of the peptide does not shift the internal protonation equilibrium between both MII species. In Figure 4B, we show in addition the infrared difference spectra of the formation of MII_{PSB} both in the presence and in the absence of peptide. The resulting double-difference spectrum with the distinct amide I and II patterns around 1650 and 1550 cm^{-1} reflects the formation of the MII−peptide complex and corresponds to those reported in related studies with transducin-derived peptides (*29*). Peptide binding spectra with similar patterns and intensities were obtained over the entire pH range (from 4.5 to 8.0), with both MII_{380} and MII_{PSB} (*30*, *31*). Importantly, binding of the peptide does not change the intensity of the positive band at 1201 cm^{-1}, which will be shown below to be an indicator of the protonation state of the *all-trans*-retinal Schiff base in MII.

In the following two sections, we will show that this functional similarity between MII_{PSB} and MII_{380} is also reflected explicitly in the protein conformation as seen by infrared as well as near-UV difference spectroscopy of the two states.

Characterization of MII_{PSB} by Infrared Spectroscopy. We determined the light-induced FTIR difference spectra of rhodopsin in the presence of 100 mM NaSCN at high pH (7.0), where only MII_{380} is formed,[2] and at low pH (∼4; see Experimental Procedures), where the photoproduct is predominantly MII_{PSB} (Figure 5A). In the difference spectra, positive bands are caused by the photoproducts while negative bands correspond to the dark state. Obviously, both difference spectra are very similar, and changes in the band pattern are restricted mainly to three regions of the spectral range: (1) around 1200 cm^{-1} in the fingerprint region of chromophore C−C vibrations, (2) around 1550 cm^{-1} in the range of the protein amide II vibrations and the chromophore C═C ethylenic stretching mode, and (3) around 1650 cm^{-1} in the range of protein amide I vibrational bands and the chromophore Schiff base C═N stretch frequency. To allow a clearer analysis of the spectral changes, we subtracted the spectra in Figure 5A to obtain the MII_{PSB} minus MII_{380} double-difference spectrum, which is shown in Figure 5B, using the negative band at 1768 cm^{-1} attributed to Asp^{83} in the dark state (*32*, *33*) for normalization. To be able to distinguish between bands that can be attributed to the protein moiety of the photoproducts and those related to the chromophore, the same procedure was repeated with rhodopsin that was labeled with ^{13}C at positions C-14 and C-15 of retinal. The double-difference spectrum of the labeled photoproducts is shown in Figure 5C. As we will show in the following, most of the spectral changes observed between MII_{380} and MII_{PSB} simply reflect an increased absorption strength of chromophore bands due to the protonation of the Schiff base and give no indication of a different protein conformation.

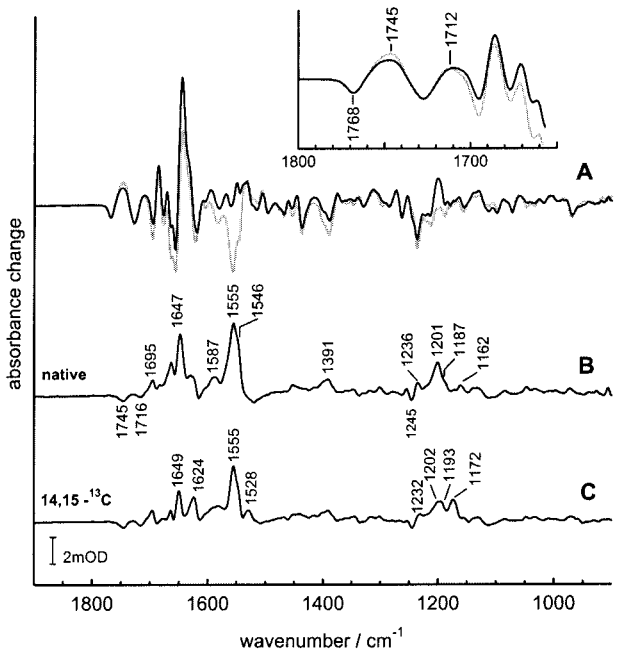

FIGURE 5: Comparison of FTIR difference spectra of both MII species. (A) Light-induced FTIR difference spectra (photoproduct minus dark state) of rhodopsin in membranes obtained in the presence of 100 mM NaSCN at 10 °C and pH 7.0 (gray line), corresponding to normal MII (MII_{380}), and at approximately pH 4.0 (black line), corresponding to MII with a protonated Schiff base (see also Experimental Procedures for sample preparation and pH adjustment). The inset shows an enlarged view in the range of protonated carboxylic acids. (B) MII_{PSB} minus MII_{380} double-difference spectrum. Difference spectra as in part A were normalized to the negative band at 1768 cm^{-1} and subtracted. In the double-difference spectrum, positive bands correspond to MII_{PSB} and negative bands to MII_{380}. (C) As for part B, but with rhodopsin regenerated with ^{13}C-labeled retinal (at C-14 and C-15). The spectra in parts B and C are the average of each two experiments. The wavenumber assignment of all spectra is based on their second derivative.

The difference bands around 1200 cm^{-1} in the fingerprint region of the double-difference spectra are easiest to interpret. Obviously, all large bands in parts B and C of Figure 5 are positive and can therefore be attributed to MII_{PSB}. It is a general property of retinal Schiff bases and retinal proteins that vibrational modes of unprotonated Schiff bases absorb only weakly compared to those of protonated Schiff bases (*34*). From the chromophore-related bands, we will therefore mainly see those arising from MII_{PSB}, which are in the chosen representation positive. All major bands in the fingerprint region can be attributed to specific C−C stretching modes of the protonated *all-trans* chromophore of MII_{PSB}, based upon results from resonance Raman experiments with rhodopsin and model Schiff bases of retinal (*35*−*37*). The band pattern can be best described by assigning the bands at 1236 (1232 cm^{-1}), 1201 (1202 cm^{-1}), 1187 (1172 cm^{-1}), and 1162 cm^{-1} (∼1162 cm^{-1}) (the values in parentheses are the respective wavenumbers for MII_{PSB} with ^{13}C-labeled pigment) to the C-12−C-13, C-8−C-9, C-14−C-15, and C-10−C-11 stretch modes as the principal stretch components, respectively, each coupled to other stretch and CH

[2] It was reported previously that the pK_a of the MI ⇌ MII equilibrium is shifted to higher values in FTIR samples involving drying and rehydration of membranes (*31*) than in solution samples. While in suspension samples there is a significant MI contribution at pH 7.0 and 10 °C, in the presence of 100 mM NaSCN (see Figure 5A), there is still a pure MII photoproduct in FTIR sandwich samples.

rocking modes. The band positions and the assignments of the vibrational modes are in agreement with the Raman data.

The strong band at 1555 cm^{-1} presumably consists mainly of the ethylenic stretch mode of the protonated chromophore. The position of this band was also assayed with iodide, nitrate, and bromide and seems to be independent of the anion species (data not shown). This is consistent with the visual absorption maximum of MII_{PSB} being seemingly independent of the anion species, as the ethylenic stretch mode and the visual absorption maximum of the chromophore were shown to be strongly correlated (*37*). As suggested in Figure 5B, the ethylenic stretch mode is likely to be composed of two components, the second, smaller band absorbing around 1546 cm^{-1} and shifting to 1528 cm^{-1} in the ^{13}C-labeled pigment. The region around 1650 cm^{-1} is difficult to interpret, as it contains not only the C═N vibration of the Schiff base but also a strong background absorption due to the amide I bands of the protein and of the OH bending mode of water, which introduces some noise into the single spectra. Nevertheless, the data are best described by assigning the 1647 cm^{-1} band to a superposition of the C═N stretch mode of the chromophore in MII_{PSB} and a small amide I contribution, of which the first is downshifted to 1624 cm^{-1} upon labeling with ^{13}C.

Importantly, the bands around 1700 cm^{-1} and above are conserved in MII_{380} and MII_{PSB}. In particular, the positive band at 1712 cm^{-1} is very similar in both species. This band is attributed to the protonation of Glu^{113} in MII (*38*), which forms the counterion to the protonated Schiff base in the dark state (*5*, *6*). From this, we can conclude that Glu^{113} becomes protonated in both MII_{380} and MII_{PSB} and that the positive charge of the Schiff base in MII_{PSB} must therefore be stabilized in a manner different from that for the dark state. It is tempting to postulate that an exogenous anion is adopting the role of the new counterion by binding to or near the Schiff base of MII_{PSB}. We will address this issue below. Even if Glu^{113} is protonated in both MII_{380} and MII_{PSB}, we would expect its immediate environment to be slightly changed upon introduction of the putative proton/anion charge pair. Indeed, the position of the positive difference band attributed to Glu^{113} is not exactly the same in both species. Instead, it is slightly shifted to lower frequencies in MII_{PSB}, suggesting stronger hydrogen bonding of Glu^{113} due to the presence of the additional charge pair (inset of Figure 5). The small negative band located at 1745 cm^{-1} can possibly be ascribed to protonated Glu^{122} (*32*), which experiences a slight decrease in the absorption of MII_{PSB} compared to that of MII_{380}, possibly mediated by changes in the electronic structure of the chromophore due to its protonation.

We can therefore summarize that the major differences between MII_{380} and MII_{PSB} in the infrared are mainly due to changes in chromophore bands, which are intrinsically sensitive to the protonation state of the Schiff base, and are fully compatible with a conformation identical for both states.

Characterization of the MII_{PSB} Conformation by UV Absorbance Changes. It was shown previously that the formation of the active state MII involves a change in the relative disposition of helices 3 and 6 within the helix bundle (*39*−*41*), which can be monitored by changes in the UV absorbance of Trp^{126} on helix 3 and Trp^{265} on helix 6 serving as sensitive probes for the involved structural changes (*42*, *43*). MII_{380} and MII_{PSB}, the latter stabilized by either chloride or thiocyanate, produce the same UV difference pattern upon formation, which is different from that obtained for MI (data not shown). The patterns correspond to the published spectra for MII_{380}, which were shown to be identical to that of the active state with the protonated Schiff base of the E113A/A117E double mutant (*42*). They also correspond to the UV difference spectra obtained for the MII photoproduct of the artificial pigment 9-demethylrhodopsin (R. Vogel and F. Siebert, unpublished results), which also has a partially protonated Schiff base.

This shows, in full agreement with the FTIR and peptide binding data, that a protonated Schiff base is compatible with an active conformation of the whole protein, as long as certain other requirements are met, e.g., breaking of the constraining salt bridge between Glu^{113} and the Schiff base by neutralization of the residue at position 113 (*19*, *44*).

Proton and Anion Binding Model. In this section, we will describe a model for the Schiff base protonation equilibrium in MII, which is amenable for an analytical treatment. The rationale of this model is, first, that the proton that binds to the Schiff base is an exogenous proton, which enters from the solvent, as is evident from the titration curves and also the FTIR data. Second, the pK_a of the Schiff base in MII is dependent on the presence of a suitable negative charge, which may stabilize its protonated form. Glu^{113}, which is the counterion to the protonated Schiff base in the dark state and MI of rhodopsin, cannot serve as a counterion to MII_{PSB}, as is evident from the infrared spectroscopic data. We therefore suggested above that an endogenous anion may balance the positive charge of the Schiff base in MII_{PSB}.

In the proposed 2 × 2 model (Scheme 1), either proton H^+ or anion A^- binds first to or near the Schiff base of MII and forms the species MII·H^+ or MII·A^-, respectively, where MII alone represents in this notation the unligated MII state with a deprotonated Schiff base. These species are then stabilized by subsequent binding of their counterpart to form the fully ligated state MII·H^+·A^- species. As we show in the Supporting Information, the present experimental data do not support any substantial population of the semiligated MII·H^+ and MII·A^- states. When these transition states are neglected, the 2 × 2 model can be reduced to a two-state model, in which it is sufficient to consider only the unligated and the fully ligated states, MII and MII·H^+·A^-, respectively, and to treat the formation of the MII·H^+·A^- state as the formal binding of a proton and anion as a pair.

In this reduced model (eq B3 in the Supporting Information), we can calculate the amount of MII with protonated Schiff base starting from the reaction scheme

Scheme 1

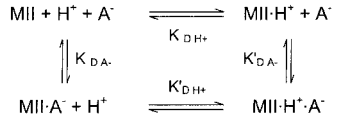

$$MII{\cdot}H^+{\cdot}A^- \rightleftharpoons MII + H^+ + A^- \quad (1)$$

and the corresponding equation for dissociation

$$\frac{[MII][H^+][A^-]}{[MII{\cdot}H^+{\cdot}A^-]} = K_D \quad (2)$$

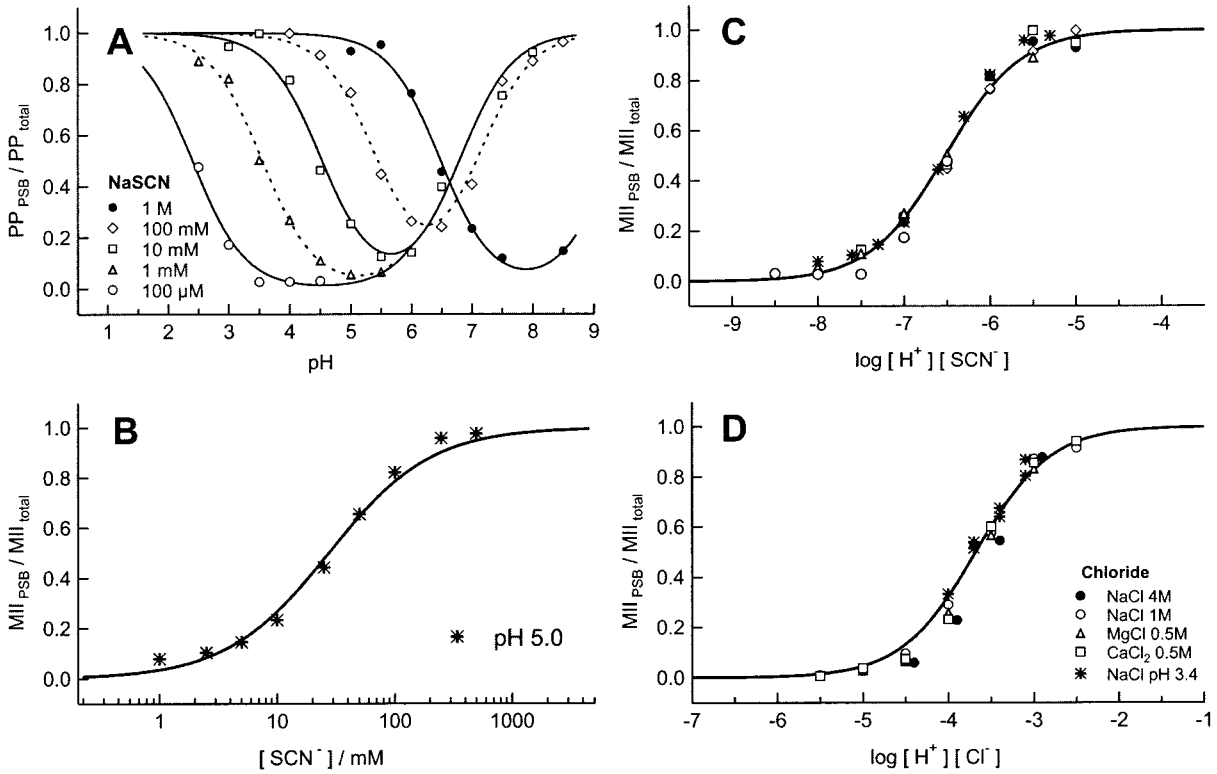

FIGURE 6: Dependence of the protonation state of the Schiff base in MII on anion and proton concentration. (A) The amount of photoproduct with a protonated Schiff base (PP_{PSB}, either MII_{PSB} at acidic pH or MI at alkaline pH) was determined via the dependence of pH at different NaSCN concentrations with pigment in membranes at 10 °C (2 mM buffer for 100 μM and 1 mM NaSCN, and 20 mM otherwise). The lines are fits to a Henderson−Hasselbalch equation with two pK_a values for the $MII_{PSB} \rightleftharpoons MII_{380}$ and $MII_{380} \rightleftharpoons$ MI transitions (see Table 2 for the determined values). (B) The amount of MII_{PSB} was determined as described for panel A, but via the dependence of the thiocyanate concentration at a fixed pH of 5.0. (C) Data from panels A and B plotted via the dependence of the product of proton and anion concentration. The solid line is a least-squares fit to eq 3 (best fit, K_D = 310 nM and r^2 = 0.98), and data points from the alkaline side of the titration curves in panel A containing MI contributions were omitted. (D) As for panel C, but with different chloride salts assayed with purified pigment in dodecyl maltoside. The solid line is a fit to eq 3 (K_D = 220 μM and r^2 = 0.97).

With the normalization [MII] + [MII·H^+·A^-] = 1, we obtain

$$\frac{MII_{PSB}}{MII_{380} + MII_{PSB}} = [MII\cdot H^+\cdot A^-] = \frac{[H^+][A^-]}{[H^+][A^-] + K_D} = \frac{10^{-pH}[A^-]}{10^{-pH}[A^-] + K_D} \quad (3)$$

where K_D is the overall dissociation constant for the proton and anion and defined as $K_D = K_{DH^+}K'_{DA^-}$ (eq B4 in the Supporting Information). To correlate K_D with the experimental data, we can calculate

$$K_D = [H^+][A^-]\frac{1 - [MII\cdot H^+\cdot A^-]}{[MII\cdot H^+\cdot A^-]} = 10^{-pH}[A^-]\left(\frac{1}{[MII\cdot H^+\cdot A^-]} - 1\right)$$

$$\overset{pH=pK}{=} 10^{-pK_a}[A^-] \quad (4)$$

where pK_a denotes the apparent pK_a of the transition between MII_{380} and MII_{PSB} at a fixed anion concentration (at pH = pK_a, [MII·H^+·A^-] = 0.5).

To test the validity of this model, which expresses the influence of anion concentration and pH on the formation of MII_{PSB} in a single, anion specific dissociation constant K_D, we experimentally determined the influence of an anion species over a wide range of pHs and anion concentrations. We chose thiocyanate as the model anion for practical reasons, as it binds comparatively easily to MII and does therefore not require an extremely low pH. As we will show later, the results also apply to other anions such as chloride.

As can be seen in Figure 6A, where we varied the pH and left the anion concentration fixed, the pK_a of the transition from MII_{380} to MII_{PSB} decreases each time by approximately one pK_a unit upon reduction of the anion concentration to $^1/_{10}$ of the initial value. At alkaline pH, we have an additional transition to a different species with a protonated Schiff base, which is MI also being in a pH-dependent equilibrium with MII (*7*). Interestingly, the pK_a of the conformational transition to MI (denoted as pK_2) also shows some salt dependence, although only at higher concentrations of thiocyanate (Table 2). This effect of salts on the conformational equilibrium between MI and MII was shown previously (*45*) and was in a subsequent study assigned to the Hofmeister effect (*46*), and in particular to a preferential binding of chaotropic ions to the protein in the MII conformation. To account in our analysis also for the transition from MII to MI, the solid lines in Figure 6A are fits to a sum of two Henderson−Hasselbalch equations with different pK_a values (see Experimental Procedures). The fitted values for both pK_a values are shown in Table 2.

In Figure 6B, we fixed the pH at 5.0 and varied the anion concentration. The solid line is a fit to eq 3. In Figure 6C, the data from panels A and B (except for those containing

Table 2: pK_a Values for the $MII_{PSB} \rightleftharpoons MII_{380}$ and $MII \rightleftharpoons MI$ Transitions[a]

salt	pK_1 ($MII_{PSB} \rightleftharpoons MII_{380}$)	pK_2 ($MII \rightleftharpoons MI$)
1 M NaSCN	6.5	>9
100 mM NaSCN	5.4	7.1
10 mM NaSCN	4.5	6.8
1 mM NaSCN	3.5	6.9
100 μM NaSCN	2.4	6.8
20 mM buffer (BTP/MOPS)	−	6.9

[a] All data were determined with pigment in membranes at 10 °C. The pK_a values are from least-squares fits of the data of Figure 6A and other data, and the error for the pK_a values is estimated to be ±0.15.

MI) are plotted altogether in dependence of the product $[H^+][A^-]$. Obviously, they all superimpose to a single titration curve. The solid line is again a fit to eq 3 with a K_D of 310 nM for thiocyanate. Similar experiments were carried out with different chloride salts and purified rhodopsin in detergent (Figure 6D). Also in this case, all titration curves superimpose to a single curve when plotted over the concentration product $[H^+][A^-]$. In the case of chloride, the K_D is 220 μM. The K_D values for other anions are shown with the respective pK_a values for 1 M anion in Table 1.

These experiments clearly show that formation of MII_{PSB} requires the stoichiometric binding of one proton and one anion to MII to form the $MII \cdot H^+ \cdot A^-$ species. In the last section, we will try to further characterize the binding process itself by monitoring characteristic changes in the vibrational stretch mode of thiocyanate upon binding.

Changes of the Vibrational Frequency of Thiocyanate upon Binding to MII. We chose thiocyanate as a probe for changes of its hydrogen bonding properties upon binding as it has in aqueous solution a strong and narrow absorption band at 2065 cm^{-1}, a range where there are no other overlapping bands of either protein or chromophore. Chaotropic ions such as thiocyanate are known to bind to the peptide bonds and other groups of proteins, thereby inducing a partial unfolding of the native structure (*47*, *48*). It is commonly accepted that the photoactivation of rhodopsin is accompanied by conformational changes of its cytoplasmic domain (*49*), which may also be interpreted as a partial unfolding of otherwise ordered structures (*50*). This view is also supported by the observation that soluble constructs of this domain lacking the stabilizing transmembrane core of the protein are also able to form an active state (*51*). We therefore expect to see changes in the vibrational properties of thiocyanate during the transition from the dark state to MII_{380}. To distinguish these changes from those arising from the expected stronger binding to MII_{PSB}, we determined the light-induced FTIR difference spectrum of rhodopsin in the presence of thiocyanate at neutral pH, where only MII_{380} is formed, and compared it to the spectrum observed at low pH, where MII_{PSB} is predominantly formed (Figure 7). In the case of MII_{380}, a difference pattern corresponding to a slight downshift of the thiocyanate stretch mode can be observed, which is in line with an increased level of binding of thiocyanate to the peptide moiety of the protein in MII compared to that in the dark state. A similar downshift associated with a band narrowing is observed if thiocyanate is dissolved in the aprotic solvent DMSO, while there is a splitting into several bands absorbing between 2100 and 2025 cm^{-1} in ethanol (data not shown). Upon formation of MII_{PSB}, the pattern and

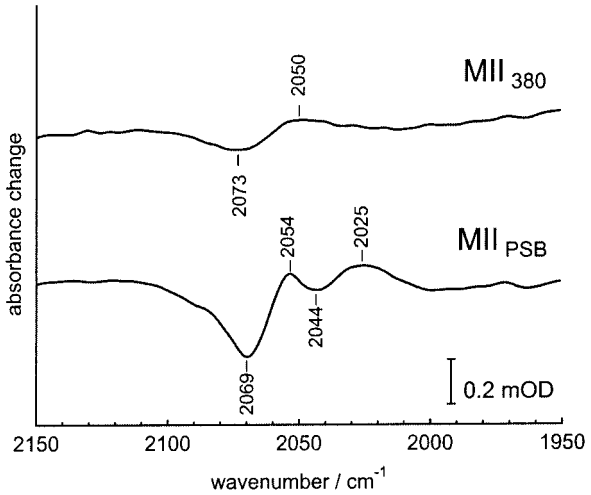

FIGURE 7: Binding of thiocyanate to the Schiff base in MII. Changes of the SCN^- stretching mode upon formation of MII were followed with light-induced FTIR difference spectroscopy in the presence of 100 mM thiocyanate at pH 7.0 (MII_{380}) and at approximately pH 4 (MII_{PSB}). The experiments were carried out at 10 °C with pigment in membranes, and the spectra are the average of each two experiments and correspond otherwise to those in Figure 5A.

intensity of the bands change considerably, giving rise to two negative peaks at 2069 and 2044 cm^{-1} and two positive peaks at 2054 and 2025 cm^{-1} in the difference spectrum. Such a pattern is in agreement with a considerable change in the hydrogen bonding of the thiocyanate anion upon binding near the protonated Schiff base.

DISCUSSION

The pK_a values of the protonated Schiff base and its counterion in retinal proteins are an intriguing problem (*14*). It was demonstrated recently that in rhodopsin the pK_a of the protonated Schiff base of retinal is above 16 and thus remarkably elevated relative to that in solution (7.2) (*15*). It was proposed that this unusual pK_a can be attributed to a special stabilization of the protonated Schiff base−counterion pair by a bridging water molecule (*16*). In the unphotolyzed state, the protonated Schiff base and its counterion establish a geometry suitable for a very efficient hydrogen bonding network with the water molecule which stabilizes the ion pair. Following retinal isomerization and the subsequent protein conformational changes, the protonated Schiff base−counterion geometry is altered and the special effect of the water molecule is diminished, leading to a proton transfer from the Schiff base to its counterion. Neutralization of the counterion in MII is accompanied by a very low pK_a of the Schiff base, which is <2.5 in the absence of anions, as revealed in the study presented here.

Deprotonation of the Schiff base is commonly considered to be a key step in the activation of rhodopsin after photoexcitation. Recently, however, modified pigments were found that are able to form an active state without deprotonation of the Schiff base. In some of these pigments, glutamic or aspartic acids were introduced at positions different from that of the native counterion, which then formed the counterion to the protonated Schiff base in the activated receptor (*19*). In one pigment with an artificial chromophore, the positively charged Schiff base was pre-

sumably stabilized solely by internal water (*20*). In all of these photoproduct states, the pK_a of the Schiff base is therefore increased by the presence of countercharges or, in one case, possibly by the increased polarity of the Schiff base environment.

In this study, we show for the first time that a photoproduct with an active state conformation and a protonated Schiff base can also be stabilized in native rhodopsin solely by the presence of suitable anions. From the presented infrared spectra, it is evident that the anion-induced stabilization of this MII_{PSB} state does not interfere with charge neutralization of Glu^{113} upon activation, which was shown to proceed likely via proton transfer from the Schiff base (*38*). Compared to that of MII_{380}, the formation of this novel photoproduct MII_{PSB} therefore involves an uptake of an additional solvent proton directly to the Schiff base. This, however, would introduce an energetically unfavorable net charge in the protein interior, unless a solute anion is likewise being bound. We could show that this anion binds with a stoichiometry of 1, as is evident from the perfect agreement of the experimental data with model calculations over a concentration range of 4 orders of magnitude for the anion and 5 orders of magnitude for the proton, both limited by the stability of the protein at low pH or high salt concentration and by its pH-dependent transition to MI at alkaline pH. For a further localization of the anion binding site within the protein, it may be helpful to consider again the rhodopsin mutants G90D and E113A/A117E, where the newly introduced or the shifted counterion stabilizes a protonated Schiff base in MII as well. With regard to these mutants, an anion binding site close to the respective residues within the protein seems possible.

The stabilization of MII_{PSB} is highly selective with regard to the anion species. The experimentally obtained anion specific dissociation constant for the proton varies from the millimolar range for sulfate to ~300 nM in the case of thiocyanate. The order of the dissociation constants of the anions is as follows: sulfate > chloride > bromide > nitrate > iodide > thiocyanate. Interestingly, this order follows the strength of ion−water interactions for each anion in aqueous solution as determined by affinity chromatography (*25*, *52*), as expressed in the Jones−Dole viscosity *B* coefficient (*52*, *53*), which relates the strength of ion−water interactions to the viscosity of aqueous salt solutions (*54*), or as found for the anion dehydration energies (*55*). In particular for the halides, the order is also consistent with their ability to permeate phospholipid bilayers (*56*). Importantly, similar anion selectivities were recently reported for the CFTR chloride channel (*57*) and for anion binding in a green fluorescent protein mutant (*58*), and were in both cases interpreted in terms of anion dehydration energies. We can therefore conclude that the dissociation constant and thus the ability of an anion species to stabilize MII_{PSB} are largely determined by its weakness of hydration and thus reflect simply its ability to partition into the much less polar environment of the protein interior.

An interesting observation is the apparent lack of an influence of the anion species on the visible absorption maximum λ_{max} of MII_{PSB}, while there is a strong influence in the dark state of rhodopsin counterion mutants (*17*, *18*). It is well-known that in nonpolar solvents the absorption maximum of protonated retinal Schiff bases is influenced by the counterion's nature due to direct electrostatic interaction between the two charges which, in turn, is influenced by the distance between the two. In polar solvents, both charges are well solvated, thus abolishing the effect of the anion nature. The absorption maximum of the retinal-protonated Schiff base in solvents such as methanol is 440 nm and well blue shifted relative to the absorption observed in MII_{PSB}. However, it was observed that the absorption is red shifted in certain polar solvents, which are capable of efficient solvation of the anion but interact only relatively weakly with the positively charged Schiff base (*59*). In analogy, we propose that in MII_{PSB} the anion is partially solvated by water molecules, thereby reducing the effect of the anion nature on the absorption maximum, but still retaining its capability to increase the Schiff base pK_a. A red-shifted absorption compared to that of a protonated retinal Schiff base in aqueous solution is observed due to weak solvation of the protonated Schiff base linkage.

In summary, we have shown in this study that not only in several rhodopsin mutants but also in native rhodopsin an active protein conformation and a protonated retinal Schiff base are compatible as long as the constraining salt bridge between the Schiff base and Glu^{113} on helix 3 is broken. The intrinsic pK_a of the retinal Schiff base in rhodopsin sensitively depends on the polarity of its immediate environment and may therefore be considerably increased by the presence of suitable anions which may partition into the less polar protein environment. Binding of anions within the protein is therefore not restricted to the archaeal ion pumps, but it also seems to play a major role in determining the properties of some other, visual pigments (*2*, *60*), and may be a general mechanism for modulating the polarity in proteins (*53*).

ACKNOWLEDGMENT

We thank B. Mayer, W. Sevenich, K. Zander, and P. Merkt for their excellent technical assistance, J. Lugtenburg for the isotopically labeled retinal, and Prof. W. Haehnel for the peptide synthesis.

SUPPORTING INFORMATION AVAILABLE

Derivation, analysis, and interpretation of the extended binding model (2 × 2 model). This material is available free of charge via the Internet at http://pubs.acs.org.

REFERENCES

1. Sakmar, T. P. (1998) *Prog. Nucleic Acid Res. Mol. Biol. 50*, 1−34.
2. Shichida, Y., and Imai, H. (1998) *Cell. Mol. Life Sci. 54*, 1299−1315.
3. Schertler, G. F. X., Villa, C., and Henderson, R. (1993) *Nature 262*, 770−772.
4. Palczewski, K., Kumasaka, T., Hori, T., Behnke, C. A., Motoshima, H., Fox, B. A., Le Trong, I., Teller, D. C., Okada, T., Stenkamp, R. E., Yamamoto, M., and Miyano, M. (2000) *Science 289*, 739−745.
5. Sakmar, T. P., Franke, R. R., and Khorana, H. G. (1989) *Proc. Natl. Acad. Sci. U.S.A. 86*, 8309−8313.
6. Zhukovsky, E. A., and Oprian, D. D. (1989) *Science 246*, 928−930.
7. Matthews, R. G., Hubbard, R., Brown, P. K., and Wald, G. (1963) *J. Gen. Physiol. 47*, 215−240.
8. Hofmann, K. P. (1986) *Photobiochem. Photobiophys. 13*, 309−327.

9. Emeis, D., Kühn, H., Reichert, J., and Hofmann, K. P. (1982) *FEBS Lett. 143*, 29−34.
10. Hamm, H. E., Deretic, D., Arendt, A., Hargrave, P. A., König, B., and Hofmann, K. P. (1988) *Science 241*, 832−835.
11. Helmreich, E. J. M., and Hofmann, K. P. (1996) *Biochim. Biophys. Acta 1286*, 285−322.
12. Blatz, P. E., Mohler, J. H., and Navangul, H. V. (1972) *Biochemistry 11*, 848−855.
13. Livnah, N., and Sheves, M. (1993) *J. Am. Chem. Soc. 115*, 351−353.
14. Ebrey, T. G. (2000) *Methods Enzymol. 315*, 196−207.
15. Steinberg, G., Ottolenghi, M., and Sheves, M. (1993) *Biophys. J. 64*, 1499−1502.
16. Gat, Y., and Sheves, M. (1993) *J. Am. Chem. Soc. 115*, 3772−3773.
17. Nathans, J. (1990) *Biochemistry 29*, 9746−9752.
18. Sakmar, T. P., Franke, R. R., and Khorana, H. G. (1991) *Proc. Natl. Acad. Sci. U.S.A. 88*, 3079−3083.
19. Fahmy, K., Siebert, F., and Sakmar, T. P. (1995) *Biophys. Chem. 56*, 171−181.
20. Vogel, R., Fan, G. B., Sheves, M., and Siebert, F. (2000) *Biochemistry 39*, 8895−8908.
21. Fahmy, K., Siebert, F., and Sakmar, T. P. (1994) *Biochemistry 33*, 13700−13705.
22. Nakagawa, M., Iwasa, T., Kikkawa, S., Tsuda, M., and Ebrey, T. G. (1999) *Proc. Natl. Acad. Sci. U.S.A. 96*, 6189−6192.
23. Longstaff, C., Calhoon, R. D., and Rando, R. R. (1986) *Proc. Natl. Acad. Sci. U.S.A. 83*, 4209−4213.
24. Ganter, U. M., Longstaff, C., Pajares, M. A., Rando, R. R., and Siebert, F. (1991) *Biophys. J. 59*, 640−644.
25. Collins, K. D. (1995) *Proc. Natl. Acad. Sci. U.S.A. 92*, 5553−5557.
26. Ganter, U. M., Schmid, E. D., Perez-Sala, D., Rando, R. R., and Siebert, F. (1989) *Biochemistry 28*, 5954−5962.
27. DeGrip, W. J. (1982) *Methods Enzymol. 81*, 197−207.
28. Martin, E. L., Rens-Domiano, S., Schatz, P. J., and Hamm, H. E. (1996) *J. Biol. Chem. 271*, 361−366.
29. Fahmy, K. (1998) *Biophys. J. 75*, 1306−1318.
30. Nishimura, S., Kandori, H., and Maeda, A. (1998) *Biochemistry 37*, 15816−15824.
31. Bartl, F., Ritter, E., and Hofmann, K. P. (2000) *FEBS Lett. 473*, 259−264.
32. Fahmy, K., Jäger, F., Beck, M., Zvyaga, T. A., Sakmar, T. P., and Siebert, F. (1993) *Proc. Natl. Acad. Sci. U.S.A. 90*, 10206−10210.
33. Rath, P., DeCaluwe, L. L., Bovee-Geurts, P. H., DeGrip, W. J., and Rothschild, K. J. (1993) *Biochemistry 32*, 10277−10282.
34. Siebert, F., and Mäntele, W. (1980) *Biophys. Struct. Mech. 6*, 147−164.
35. Palings, I., Pardoen, J. A., van den Berg, E. M., Winkel, C., Lugtenburg, J., and Mathies, R. A. (1987) *Biochemistry 26*, 2544−2556.
36. Smith, S. O., Myers, A. B., Mathies, R. A., Pardoen, J. A., Winkel, C., van den Berg, E. M., and Lugtenburg, J. (1985) *Biophys. J. 47*, 653−664.
37. Doukas, A. G., Aton, B., Callender, R. H., and Ebrey, T. G. (1978) *Biochemistry 17*, 2430−2435.
38. Jäger, F., Fahmy, K., Sakmar, T. P., and Siebert, F. (1994) *Biochemistry 33*, 10878−10882.
39. Sheikh, S. P., Zvyaga, T. A., Lichtarge, O., Sakmar, T. P., and Bourne, H. R. (1996) *Nature 383*, 347−350.
40. Farrens, D. L., Altenbach, C., Yang, K., Hubbell, W. L., and Khorana, H. G. (1996) *Science 274*, 768−770.
41. Dunham, T. D., and Farrens, D. L. (1999) *J. Biol. Chem. 274*, 1683−1690.
42. Lin, S. W., and Sakmar, T. P. (1996) *Biochemistry 35*, 11149−11159.
43. Rafferty, C. N. (1979) *Photochem. Photobiol. 29*, 109−120.
44. Robinson, P. R., Cohen, G. B., Zhukovsky, E. A., and Oprian, D. D. (1992) *Neuron 9*, 719−725.
45. Delange, F., Merkx, M., Bovee-Geurts, P. H., Pistorius, A. M., and DeGrip, W. J. (1997) *Eur. J. Biochem. 243*, 174−180.
46. Vogel, R., Fan, G. B., Sheves, M., and Siebert, F. (2001) *Biochemistry 40*, 483−493.
47. Baldwin, R. L. (1996) *Biophys. J. 71*, 2056−2063.
48. Timasheff, S. N. (1998) *Adv. Protein Chem. 51*, 355−432.
49. Resek, J. F., Farahbakhsh, Z. T., Hubbell, W. L., and Khorana, H. G. (1993) *Biochemistry 32*, 12025−12032.
50. Ganter, U. M., Charitopoulos, T., Virmaux, N., and Siebert, F. (1992) *Photochem. Photobiol. 56*, 57−62.
51. Abdulaev, N. G., Ngo, T., Chen, R., Lu, Z., and Ridge, K. D. (2000) *J. Biol. Chem. 275*, 39354−39363.
52. Robinson, J. B., Strottmann, J. M., and Stellwagen, E. (1981) *Proc. Natl. Acad. Sci. U.S.A. 78*, 2287−2291.
53. Collins, K. D. (1997) *Biophys. J. 72*, 65−76.
54. Stokes, R. H., and Mills, R. (1965) *Viscosity of electrolytes and related properties*, Pergamon Press, Oxford, U.K.
55. Marcus, Y. (1994) *Biophys. Chem. 51*, 111−127.
56. Paula, S., Volkov, A. G., and Deamer, D. W. (1998) *Biophys. J. 74*, 319−327.
57. Smith, S. S., Steinle, E. D., Meyerhoff, M. E., and Dawson, D. C. (1999) *J. Gen. Physiol. 114*, 799−818.
58. Jayaraman, S., Haggie, P., Wachter, R. M., Remington, S. J., and Verkman, A. S. (2000) *J. Biol. Chem. 275*, 6047−6050.
59. Baasov, T., Friedman, N., and Sheves, M. (1987) *Biochemistry 26*, 3210−3217.
60. Yuan, C., Kuwata, O., Liang, J., Misra, S., Balashov, S. P., and Ebrey, T. G. (1999) *Biochemistry 38*, 4649−4654.

BI0113667